Health Assessment of Composite Structures in Unconstrained Environments Using Partially Supervised Pattern Recognition Tools.

Emmanuel Ramasso, Vincent Placet, Rafael Gouriveau, Lamine Boubakar, Noureddine Zerhouni

Health Assessment of Composite Structures in Unconstrained Environments Using Partially Supervised Pattern Recognition Tools

Emmanuel Ramasso[1], Vincent Placet[2], Rafael Gouriveau[3], Lamine Boubakar[4], and Noureddine Zerhouni[5]

[1,3,5] *Department of Automation and MicroMechatronics Systems*
surname.name@ens2m.fr

[2,4] *Department of Applied Mechanics*
surname.name@univ-fcomte.fr

[1,2,3,4,5] *FEMTO-ST Institute, UMR CNRS 6174 - UFC / ENSMM / UTBM, 25000, Besançon, France*

ABSTRACT

The health assessment of composite structures from acoustic emission data is generally tackled by the use of clustering techniques. In this paper, the K-means clustering and the newly proposed Partially-Hidden Markov Model (PHMM) are exploited to analyse the data collected during mechanical tests on composite structures. The health assessment considered in this paper is made difficult by working in unconstrained environments. The presence of the noise is illustrated in several examples and is shown to distort strongly the results of clustering. A solution is proposed to filter out the noisy partition provided by the clustering methods. After filtering, the PHMM provides results which appeared closer to the expectations than the K-means. The PHMM offers the possibility to use uncertain and imprecise labels on the possible states, and thus covers supervised and unsupervised learning as special cases which makes it suitable for real applications.

1. INTRODUCTION

1.1. Context and motivation

The use of organic matrix composite materials has seen considerable growth in many industry sectors in the last decade. The very high specific strength and stiffness and the low-weight of carbon fibres composites has catapulted the use of these materials into the aeronautic market. Their use is also increasing in automotive and railway industries. However, challenges remain to predict their durability, their multiple failure modes over long in-service conditions, to assess the remaining lifetime and to detect damages requiring immediate repair in mobile structures. The main issue is to better understand the damage mechanisms and kinetics.

Typically the observed failure consists of inter-fibre matrix cracking, fibre breakage and a variety of interfacial failure (like fibre-matrix debonding, splitting or inter-ply delamination). These damages are almost always accompanied by releases of heat and stress-wave propagation due to microstructural changes.

Detection and analysis of acoustic emissions are powerful means for identification of damage phenomena and monitoring of their evolution (Huguet, Godin, Gaertner, Salmon, & Villard, 2002; Barr & Benzeggagh, 1994; Huguet, 2002; Momon, Godin, Reynaud, RMili, & Fantozzi, 2012; Momon et al., 2010) and generally, a standard method based on only one or several features of waves is inadequate for composite materials submitted to complex loadings (Momon et al., 2012). Pattern recognition techniques are thus considered to identify distinct types of AE-signals based on a large number of features obtained from recorded wave hits. However, the formation of AE-signal clusters highly depends on:

- The experimental configuration,
- The material,
- The geometry of the specimen,
- The existence of AE-sources not correlated to specimen failure,
- The criterion to identify the particular failure mechanisms from AE-clusters.

Recent works clearly show the assets of supervised techniques to better identify AE signals regardless of test conditions (Momon et al., 2012).

This work deals with the health assessment of tubular composite structures based on data-driven approaches. Such structures are used in many application fields, such as speed

rotors, flywheels, pressure vessels, transportation systems and so on. In these applications, many sources related to the operation of the structure can generate an acoustic activity in addition to the material deformation and degradation. The surrounding electric and electronic appliances can also generate spurious signals at level of acquisition cards used with acoustic sensors. Moreover, the stress state in these composite structures is most of the time complex (multiaxial and heterogeneous) due to the combination of in-service loads and environments. These conditions make particularly difficult the prediction of damage occurrence.

1.2. Related work on data-driven approaches for damage phenomena identification and monitoring

State of the art data-driven approches for tackling the problem of identification and monitoring of damage phenomena can be found in (Momon et al., 2012) where two families of pattern recognition approches are considered:

- Unsupervised approaches, in particular a K-means clustering algorithm.
- Supervised approaches, in particular the K-Nearest Neighbours classifier.

In unsupervised approaches, the data feed a clustering algorithm which finds out the underlying data structure. The term *unsupervised* specifies that no prior is available concerning the potential membership of a datum to a particular class (also called clusters or group). Generally, unsupervised techniques require to tune the number of possible clusters, either empirically or automatically based on a given criterion (Momon et al., 2012). Many unsupervised techniques have been developed, in particular the K-means algorithm used in (Momon et al., 2012) where the optimisation relies on the Euclidean distance which defines circle-shaped clusters. Other algorithms exist, and some are able to manage the number of clusters sequentially while relying on the Mahalanobis distance to fit ellipsoid-shaped clusters with any orientation (Serir, Ramasso, & Zerhouni, 2012).

In supervised techniques, each datum is accompanied by a label which represents the class. Data and labels are then used to train a classifier which roughly consists in finding the frontiers between the classes. Given a testing instance, the classifier infers membership degrees to all possible classes, and the class with the maximum membership can be selected. Many classifiers have been proposed in the literature, in particular the K-Nearest Neighbours (KNN) (Momon et al., 2012) which is a model-free classifier which assigns to the testing instance the most similar datum found in the training dataset.

1.3. Problem statement and contribution

Instead of considering a binary situation where one has or does not have labels of damage, we consider a more general case called *partially-supervised modelling* which consists in assuming that the prior on labels is now encoded with imprecision and uncertainty. The introduction of this soft computing part enables one to cope with variable situations:

- If the labels are precise and certain for the whole dataset, then one retrieves the *supervised* case.
- If the labels are fully imprecise and certain for the whole dataset, then one retrieves the *unsupervised* case.
- If the labels are fully imprecise and certain only for a part of the dataset but precise and certain for the other part, then one is facing a *semi-supervised* case.
- If the labels takes the form of an uncertainty measure such as a probability, a possibility or a belief mass distribution (Klir & Wierman, 1999) over the set of labels, then one is facing a *partially-supervised* case.

Therefore, the partially-supervised case is the most general situation and enlarges the binary situation (supervised or unsupervised) by considering a *soft* case. It paves the way for the development of algorithms able to manage supervised or unsupervised cases.

Partially-supervised learning was considered in several algorithms such as the K-nearest neighbours classifier (Denoeux, 1995), decision trees (Vannoorenberghe & Denoeux, 2002) and mixture models (Vannoorenberghe & Smets, 2005; Come, Oukhellou, Denoeux, & Aknin, 2009; Denoeux, 2011). In these algorithms, the uncertainty measure is represented by belief functions which generalise probabilities and set-membership approaches (Dempster, 1967; Shafer, 1976; Smets & Kennes, 1994; Smets, 1994). For prognostics and health management applications, it was exploited more recently in (Ramasso, Rombaut, & Zerhouni, 2012) where the authors proposed to combine discrete and continuous predictions.

More recently, the procedures of inference and training in Hidden Markov Models (Rabiner, 1989) were extended to the partially-supervised case and the resulting model, called a Partially-Hidden Markov Model (PHMM) (Ramasso, Denoeux, & Zerhouni, 2012), is able to perform clustering and classification. This model appears to be well-suited for data-driven identification and monitoring of damages in composites, in particular because:

PHMM manages uncertainties on labels: It is a partially-supervised technique, managing uncertainties using belief functions which is an original approach compared to the literature on composites analysis and health assessment.

PHMM considers time-dependency of features: The underlying statistical modelling takes explicitly into account the relationship between consecutive data, in opposite to previous approaches. This specificity, combined with the Evidential Expectation-Maximisation algorithm

(E2M) used to estimate the parameters in the PHMM, makes it practically more robust to initial conditions than usual methods.

PHMM is flexibility to represent distributions: The distributions of features conditionally to the damages can take various forms, in particular the mixture of Gaussians which allows to represent ellipsoid-shaped relationships between features with different orientations, in opposite to usual approches of clustering based on the Euclidean distance.

PHMM can be used for prognostics: Usual HMMs were already exploited for prognostics and the extension to PHMM can be straightforward. Note that prognostic is not considered in this paper.

Usual probabilistic HMM were exploited for damage modelling in some recent works, in particular in (Zhou et al., 2008, 2009). To our knowledge, the most related work can be found in (Wang, 2011) where imprecise probabilities are used for composite materials analysis based on HMM. Belief functions are different from imprecise probabilities (Shafer, 1976; Smets, 1994), the only mathematical link holds in the lower probability measure which represents a belief measure. The tools developed in the the theory of belief functions as considered in Shafer and Smets' mind (Shafer, 1976; Smets & Kennes, 1994) are now well recognized are suitable ones for pattern recognition and are generally developed to alleviate probabilistic assumptions.

The contribution of this paper lies in two main aspects:

- The introduction of PHMM for health assessment of composites (with the aforementioned assets).
- The proposition of a filtering approach adapted for clustering methods.
- The testing and validation of PHMM and filtering results on a real-world case.

A plot chart of the proposed methodology is given in Figure 1.

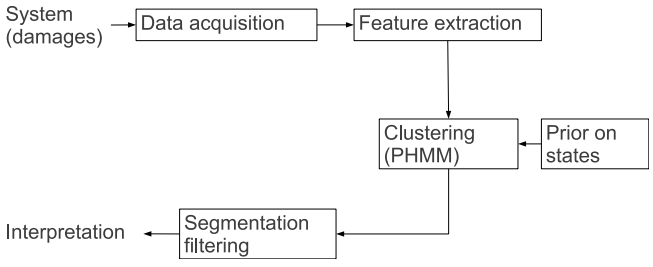

Figure 1. Plot chart of the proposed methodology.

2. EXPERIMENTS

2.1. The material

Health was assessed on composite split disks when submitted to mechanical loading. The tests were performed according to ASTM D2290 "Apparent hoop tensile strength of plastic or reinforced plastic pipe by split disk method" (Figure 2).

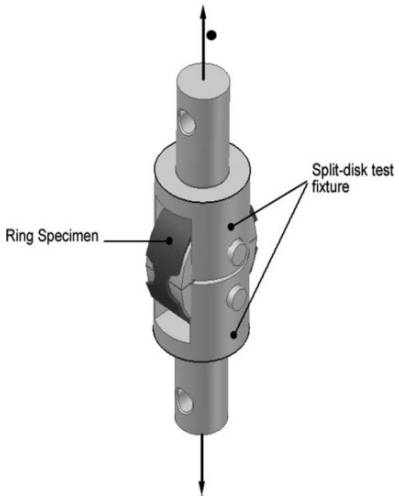

Figure 2. Experimental set-up for tensile test on split-disk specimen.

Rings were produced by cutting and machining filament-wound carbon fibre reinforced epoxy tubular structures intended for the manufacturing of flywheel rotors. Three different lay-up configurations, namely $[(90^{\circ})_6]$, $[(90^{\circ})_2/\pm 20^{\circ}/(90^{\circ})_2]$ and $[(90^{\circ})_2/\pm 45^{\circ}/(90^{\circ})_2]$ lay-ups were studied.

The transient elastic waves were recorded at the material surface using a multi-channels data acquisition system from EPA (Euro Physical Acoustics) corporation (MISTRAS Group). The system is made up of miniature piezoelectric sensors $(\mu - 80)$ with a range of resonance of $250 - 325$ kHz, preamplifiers with a gain of 40 dB and a $20 - 1000$ kHz filter, a PCI card with a sampling rate of 1 MHz and the AEWin software. The sensors were coupled on the specimen faces using a silicon grease. The calibration of the system was performed after installation of the transducers on the specimen and before each test using a pencil lead break procedure. Ambient noise was filtered using a threshold of 40 dB. The acquisition parameters: PDT (Peak Definition Time) = 60μsec; HDT (Hit Definition Time) = 120μsec and HLT (Hit Lock Time) = 300μsec were identified using preliminary measurements.

2.2. Identification of damage mechanisms and their happening under mechanical loading using Non Destructive Technique (NDT)

The damages of ring specimens caused by the mechanical loading were first identified by cautiously inspecting the inner, outer and width surfaces of the specimen following the mechanical tests. Pictures in Figure 3 and their legends precisely detail the identified damage mechanisms.

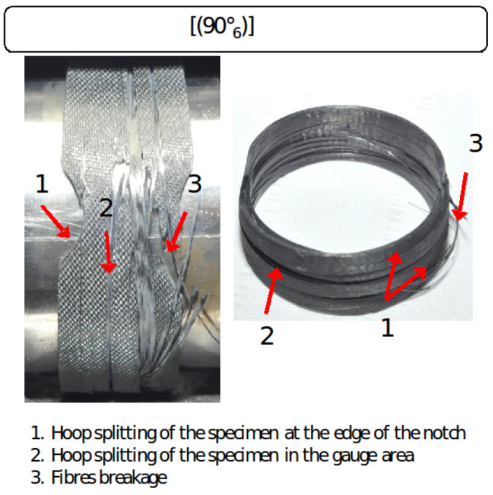

(a)

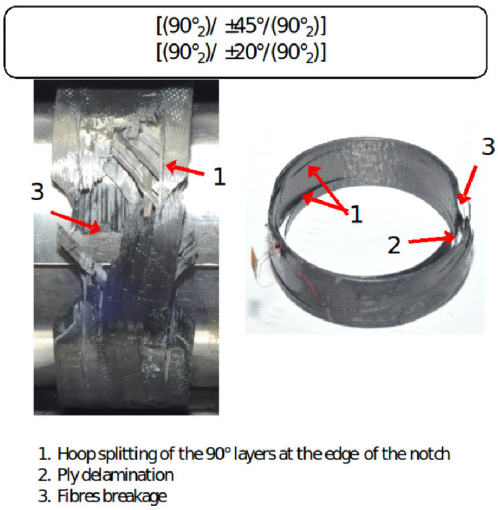

(b)

Figure 3. Photograph of the observed macro-damage on split-disk specimen after failure. Evidence of splitting in UD structures lays-up, ply delamination in multidirectional structures and fibre failures.

Some of them could have been induced by the very high level energy release at the specimen failure. To avoid any confusion and misinterpretation, some tests were also stopped just before the specimen failure (at approximately 95% of the ultimate tensile stress), and the composite observed using an optical microscope (Nikon Eclipse LV 150). These microscopic observations allowed the damage mechanisms observed from fractography images to be confirmed (Figure 4).

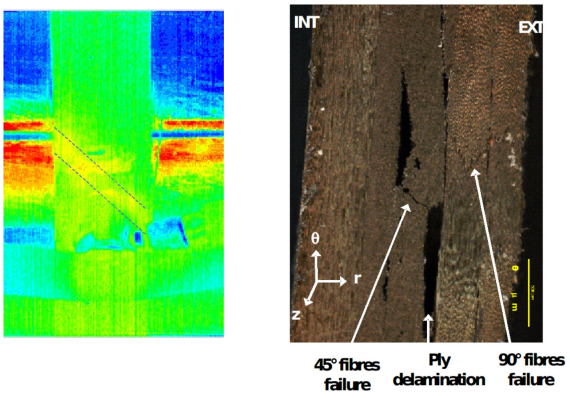

Figure 4. Micrograph of the surface of a $[(90^o)_2/\pm 45^o/(90^o)_2]$ specimen (thickness side) loaded at 95% of the maximum strength. Evidence of Matrix cracking, ply delamination and fibre breakage.

The occurrence of the damages according to the stress level were identified for each lays-up configuration using a combination of information obtained from NDT techniques, i.e. AE, IR (Infrared) thermography. A CCD Kodak Megaplus 4.2 camera was also used to record specimen pictures with a frame rate of 1 frame per second. Infrared thermography provided high resolution thermal maps as a function of loading time and allowed the damages, characterized by a heat release on the surface of the specimen, to be located (Figure 5).

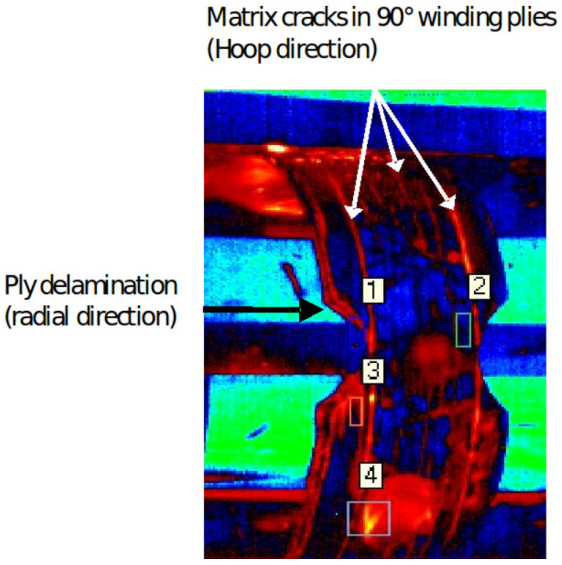

Figure 5. Infrared map during split-disk tests (specimen $[(90^o)_2/\pm 45^o/(90^o)_2]$). Evidence of matrix cracks (splitting) and radial delamination.

The used apparatus was a Mid-Wavelength InfraRed camera

with $3-5\mu$m spectral response (MWIR3 JADE from CEDIP Company). It has a focal plane array detector with 320×256 (InSb) and provides high sensitivity of less than 20mK at 300K at high speed frame rate of 150 Hz. Altair software was used to control the camera and acquire and process the infrared images. A calibration was done on the specimens in order to be able to determine absolute temperatures from the radiative measurements. It takes into account the emissivity of the material at ambient temperature and the radiation conditions of the environment. Figure 6 provides an example of the signals recorded on a $[(90^o)_2/\pm 45^o/(90^o)_2]$ specimen.

Since approximately 550MPa (20 seconds), IR images clearly show the emergence of matrix cracks, growing in the hoop direction up to the outer 90^o layers splitting. A good correlation is observed between acoustic activity and temperature increase. Each crack propagation can easily be located on the outer surface of the specimen using IR images. A temperature increase of several degrees goes with the crack propagation in this sample area. A significant increase in the absolute energy from AE of a magnitude order of 109 aJ is recorded. Since approximately 850MPa (52 seconds), a damage increase, traduced by a quick increase in temperature and in absolute energy (of about 1010aJ order) was recorded. By means of macrography images, this damage was identified to be due to bundles of fibres fracture.

The evolution of the increase in the acoustic activity and temperature at the outer surface of the specimen and the optical images allowed the different damage modes to be identified during tensile loading for each specimen. Tables 1, 2, 3 synthesised the results for each specimen family.

In the first table (Tab. 1), the damage modes and onsets as a function of mechanical stress of the UD specimen are listed. In addition to fibres breakage just before the final failure, macrocracks with specimen hoop splitting occur since 450 MPa.

The second table (Tab. 2) and the last table (Tab. 3) show that for the others stacking sequences, in addition to the hoop splitting of UD layers, inter-laminar ply delamination is detected. Experimental data do not provide enough information to clearly distinguish the onsets of each variety of interfacial failure. Ely and Hill (Ely & Hill, 1995) showed that the signal amplitude can be used as a filter criteria to distinguish fibre breakage and longitudinal splitting. Unfortunately, analysis based on only one or several of the most used parameters, such as amplitude, energy and duration as a filter criteria do not allow hoop splitting and ply delamination to be discriminated.

2.3. Identification of damage mechanisms based on acoustic emission data using pattern recognition tools

The following tests are focused on the configuration $[(90^o)_6]$.

	$[(90^o)_6]$	
Event	Loading onset (MPa)	Detected damage mode
1	$450-480$	Specimen hoop splitting
3	$1300-1610$	Fibres breakage
4	$1340-1660$	Final failure

Table 1. Damage onsets and modes as a function of lay-up configuration $[(90^o)_6]$ determined during quasi-static SD tests using NDT.

	$[(90^o)_2/\pm 45^o/(90^o)_2]$	
Event	Loading onset (MPa)	Detected damage mode
1	$470-550$	Hood splitting in 90^o layers
2	?	Ply delamination
3	$1230-1310$	Fibres breakage
4	$1250-1380$	Final failure

Table 2. Damage onsets and modes as a function of lay-up configuration $[(90^o)_2/\pm 45^o/(90^o)_2]$ determined during quasi-static SD tests using NDT.

2.3.1. Features extraction

Acoustic emission signals obtained from the acquisition board can be transformed into features which provides relevant information about the wear mechanisms.

Several features can be extracted and we refer to (Hadzor et al., 2011) for a detail overview. Figure 7 (taken from (Huang et al., 1998)) summarized the most relevant ones. There are about 22 well-known features and the most used ones are in particular: amplitude (in decibels), duration, rise time, strengh, energy, counts, counts to peak, and some frequency-based features.

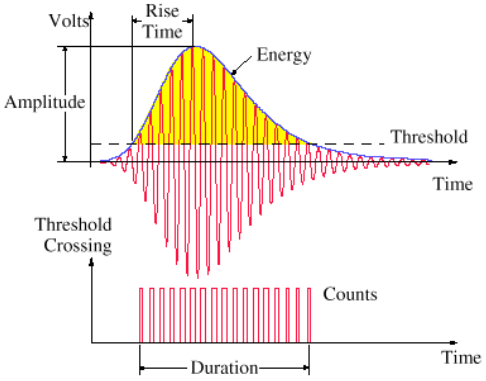

Figure 7. Features of typical AE signal.

The principal components of features were studied via a PCA with the aim of reducing the number of features by selecting the most relevant ones. Using the PCA results, 7 features were selected, accounting for 95% of the variance. An example of PCA is given in Figure 8. As underlined in several papers on AE-based materials analysis, this figure depicts that frequency-based features as well as signal energy, duration and amplitude brings most of the variance and appear as rel-

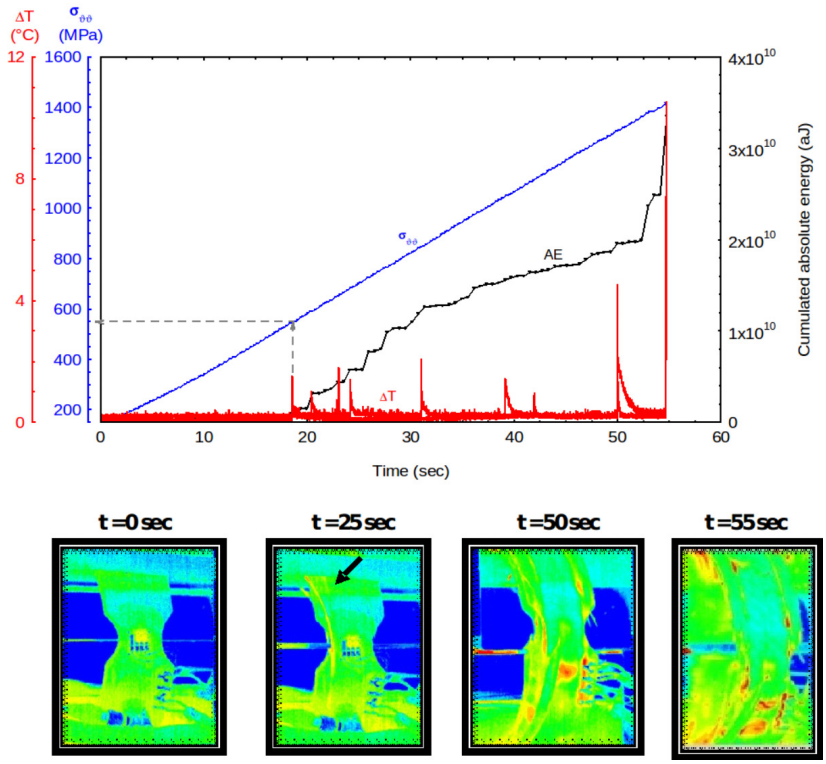

Figure 6. Evolution of the damage as a function of time during tensile tests on rings. Lays-up: $[(90^o)_2/\pm 45^o/(90^o)_2]$. Hoop stress, acoustic activity and temperature increase vs. time and infrared maps at different times.

	$[(90^o)_2/\pm 20^o/(90^o)_2]$	
Event	Loading onset (MPa)	Detected damage mode
1	$480-520$	Hoop splitting in 90^o layers
2	?	Ply delamination
3	$850-1020$	Fibres breakage
4	$900-1120$	Final failure

Table 3. Damage onsets and modes as a function for lay-up configuration $[(90^o)_2/\pm 20^o/(90^o)_2]$ determined during quasi-static SD tests using NDT.

evant features for composites analysis.

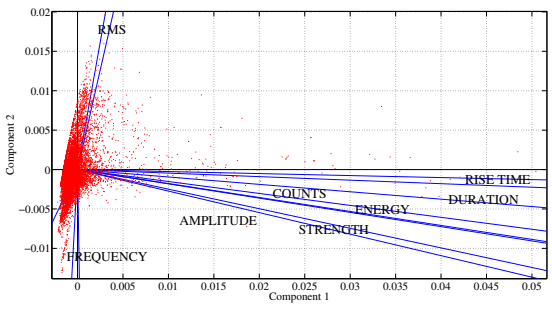

Figure 8. The principal components.

2.3.2. Noise removal

Need of noise removal When the pre-processing of data is completed (features extracted followed by a PCA), clustering algorithms can be applied in order to identify families of degrading modes. However, due to the unconstrained environment, a lot of waveforms can be registered, among which only a few represent damage mechanisms in the composite structure.

To illustrate the amount of waveforms which can be considered as false events, we simply applied the K-means clustering algorithm with $K = 10$. To cope with the dependency on the initial conditions of the K-means clustering, 200 iterations and 10 different initialisations were considered and the partition minimizing the average within-cluster distance was chosen.

The evolution of the logarithm of the cumulated sum of cluster appearance (logCSCA) along time is represented in Figure 9(a) for a configuration $[(90^o)_6]$. In this configuration, three main families of damage is generally encountered, but it is expected that each family can be represented by members with particular properties, accounting for the choice 10 clusters. This number also well illustrates the influence of noise as described hereafter.

The logCSCA is defined as follows. Let $\Omega =$

$\{1, 2, \ldots, k, \ldots, K\}$ be the set of clusters, the following matrix:

$$S(t,k) = 1 \quad \text{if cluster } k \text{ is activated at sample t} \tag{1}$$

where t is the sample index, represents the cluster appearance. The logCSCA can be computed as:

$$\log \text{CSCA}(t,k) = \log_{10} \sum_{x=1}^{t} S(x,k) \tag{2}$$

The result is depicted in Figure 9(a). This result is far from one can expect. Actually, the number of clusters located at the beginning of the experiment can not reflect a damage mechanism because this area corresponds only to the seating of the specimen in the grips. The initial portion of the stress-time curve is clearly non-linear. The material is not significantly stressed, the applied load at this point just allows the grips to be straightened. Moreover, only a few phenomenons are detected after the half of the duration of the experiment which is also unexpected since this area should be one of the most active ones.

A simple noise removal procedure enables one to obtain a much more satisfying result as depicted in Figure 9(b). The procedure is detailed below.

Noise removal procedure Since it appears difficult to automatically identify a noise waveform from other types of waveforms directly from the features, the noise removal procedure is applied after the clustering phase, i.e. in the clusters space. The noise is removed by a simple majority voting scheme in a given window with size W. The basic assumption is to consider that a mechanical phenomenon implies several consecutive waveforms with similar properties. Let S_f be the filtered matrix of cluster appearance:

$$S_f(t, k^*) = 1 \tag{3}$$

where

$$k^* = \underset{j=1}{\overset{K}{\text{argmax}}}\ \mathcal{C}_j \tag{4}$$

and

$$\mathcal{C}_j = \sum_{i=t-\frac{W}{2}}^{t+\frac{W}{2}} S(i,k) \tag{5}$$

To speed up the processing, the sliding window of size W can be moved by step equals to $P = W/2$. In this case $S_f(t^{'}, k^*) = 1, \forall t^{'} \in [t, t+P]$.

Setting up the window size At the beginning of an experiment, most of waveforms come from the straightening of the grips. This phase generates a lot of waveforms (about 20%) with small energy and small amplitude. Therefore, in this

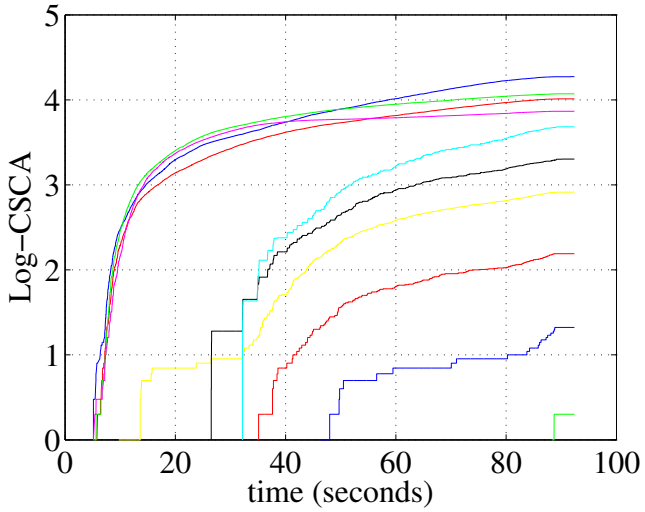

(a) K-means: Before filtering.

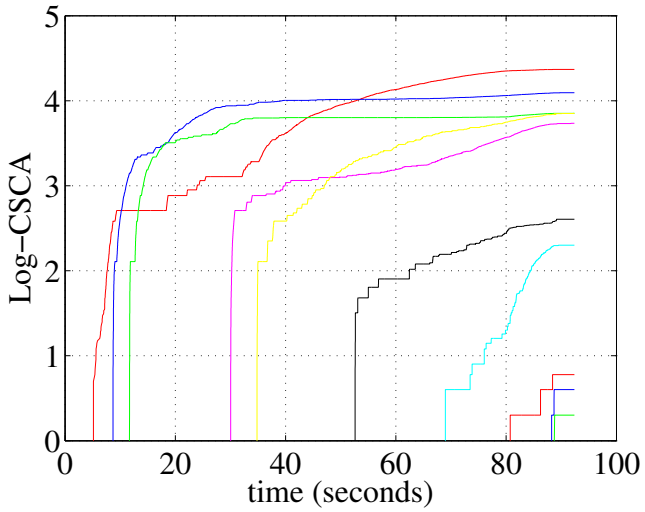

(b) K-means: After filtering.

Figure 9. Evolution of the logarithm of the cumulated sum of cluster appearance along time using the K-means with 10 clusters.

phase, the window size can be large (here chosen equal to 256 points). Then, the specimen start to be notably loaded which induces more complex mechanical phenomenons generating waveforms with particular properties until the final failure. We assume that the damages appearing along time have an increasing importance as the load increases. Therefore, in order to not filter out these potentially important phenomenons, the window size decreases along time. The decreasing rate of the window size is, for the moment, set manually, as depicted in Figure 10.

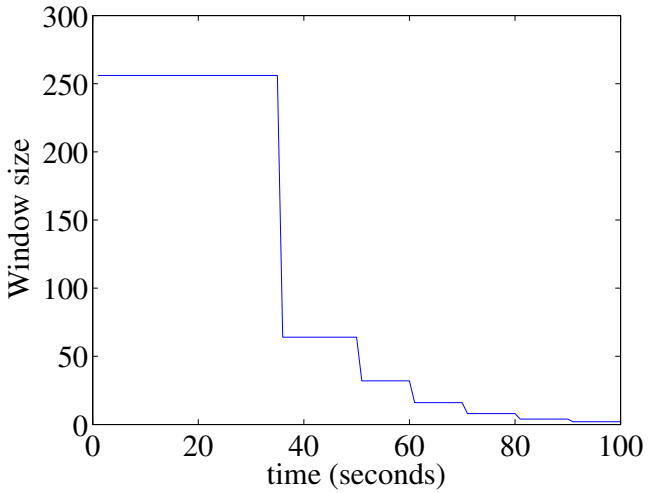

Figure 10. Evolution of the size of the window used in the noise removal procedure. The time axis represents the percentage of experiments' duration.

This noise removal procedure is illustrated in Figures 9(a)-9(b) for the K-means algorithm.

2.3.3. Clustering results

Test on $[(90^o)_6]$ with 10 states For comparison purpose (based on the aforementioned K-means results), the Partially-Hidden Markov Model (PHMM) was tuned with 10 states, 1 component for each state, using mixture of Gaussians to represent the distribution of features conditionally to the states. 10 different initialisations were used and the PHMM with the highest likelihood was selected. On the selected model, the Viterbi decoder was applied to obtain the sequence of states along time. The state sequence is then processed by the noise removal procedure. In the PHMM, two sets of partial labels were used:

- A set of labels in the 3 first seconds of the experiment, which correspond to the seating of the specimen in the grips and to the straightening of the grips.
- A set of labels in the 3 last seconds of the experiment, which correspond to the fibre breakage.

For these two areas, the plausibility of the two states was set to 1. Since other mechanical phenomenons can appear in these areas, a random noise drawn uniformly in $[0, 1]$ with $\sigma = 0.1$ was added on the labels, followed by a normalisation of the plausibilities which must be in $[0, 1]$.

Figures 11(a)-11(b) pictorially depict the clustering result before and after noise removal.

The result provided by the (post-processed) PHMM appears to be different from the K-means ones. The cluster of noise, which starts around $t = 5$ for PHMM, is well isolated by this method. This result is much more satisfying than the one obtained by the K-means which is more affected by the noise since several clusters starts very soon while there is almost no constraint. Compared to the K-means, the cluster of noise detected by the PHMM also depicts a stationary regime (around $t = 40$) which is attributed to the end of the seating of the specimen in the grips.

Moreover, the K-means seems to provide clusters with quite periodical starting points (the period seems to be close to 35 seconds on Figure 9(b)) which does not reflect the real behavior of the material. In comparison, the PHMM emphasizes that in some intervals of time, several damages appear, which seems more credible. For example, in the last 30%, several clusters have been identified, which is coherent with the fact that the material is approaching the fibres breakage and the final failure.

The results provided by the PHMM are also closer to the expectations detailed in Table 1 since three main families appear: around $t = 5$, $t = 30$ and for $t > 60$. The following tests emphasize this conclusion.

Test $[(90^o)_6]$ with 3 states The PHMM was run on the configuration $[(90^o)_6]$ with 3 states and 2 components per state and using a similar labeling process as proposed in the previous test. The number of states corresponds here to the number of expected families described in Table 1 and the number of components to different possible members to these families. Figure 12 represents the logCSDA criterion along time for this set-up. The noise removal procedure again improves the detection by separating the clusters. The first cluster still presents the stationary regime around $t = 40$ and could also includes the signature of the matrix microcracking. The second cluster may represent the hoop splitting with propagation of macrocracks, while the third may characterize the fibre breakage which, as expected, seems to generate some "jumps" in the evolution of the logCSDA.

Figure 13 also presents the results of clustering jointly with report to the mechanical stress and the cumulated energy. The positioning of the clusters is here well justified: the first cluster gathers the waveforms corresponding to the seating of the specimen in the grips where the stress is minimal, the second to possible splittings and the third to fibre breakage.

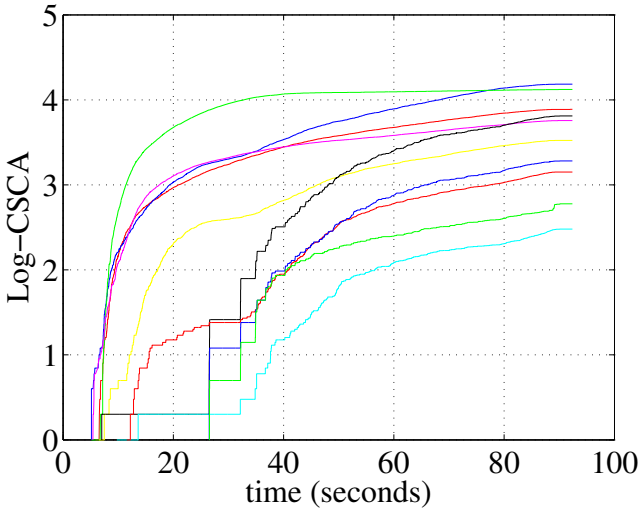

(a) PHMM: Before filtering.

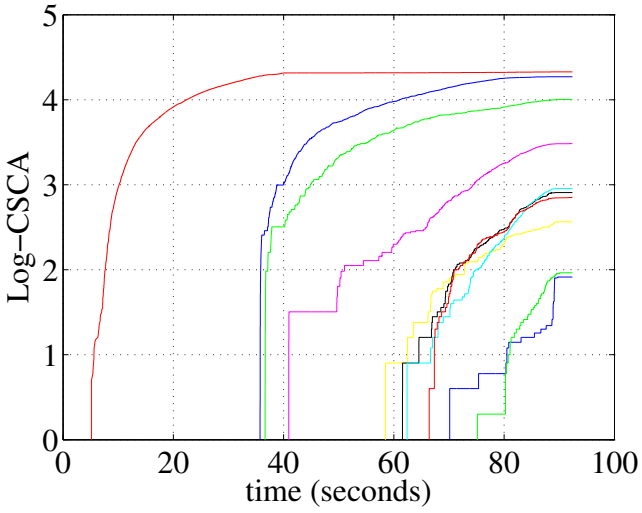

(b) PHMM: After filtering.

Figure 11. Evolution of the logarithm of the cumulated sum of cluster appearance along time using the PHMM with 10 clusters and 1 component.

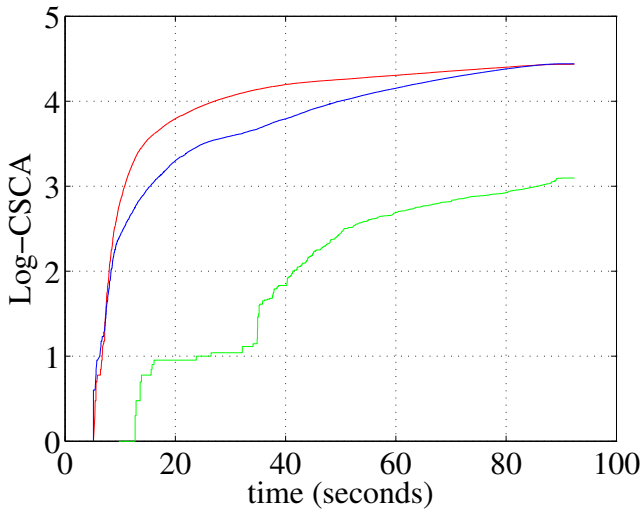

(a) PHMM: Before filtering.

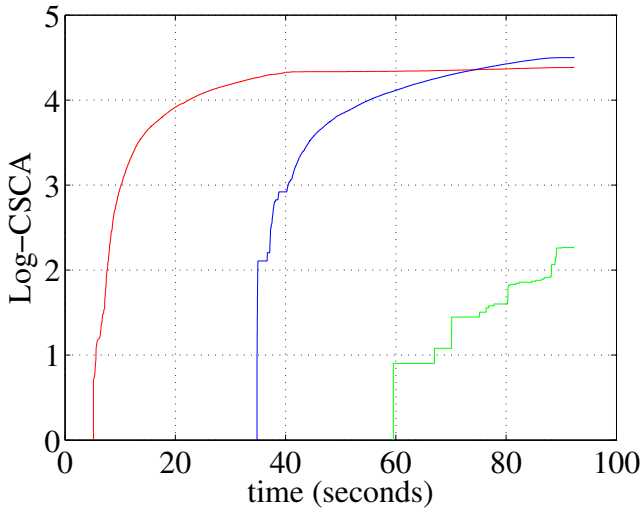

(b) PHMM: After filtering.

Figure 12. Evolution of the logarithm of the cumulated sum of cluster appearance along time using the PHMM with 3 clusters and 2 components.

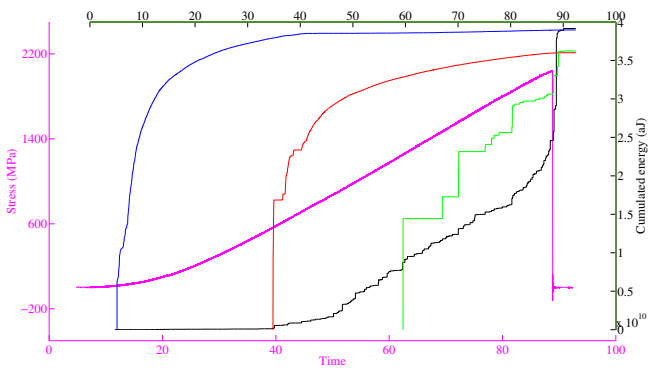

Figure 13. Viewing the results presented in Figure 12(b) jointly with the mechanical stress and the cumulated energy.

3. CONCLUSION

In this paper, we considered the problem of health assessment of composite structures in applications where the noise is present and can strongly influence the results. Considering the noise in composite structure analysis is a difficult task due to the number of data to process and to the lack of knowledge about the damage appearance and evolution. To cope with this problem, a filtering procedure working in the space of the clusters (which can be estimated by any clustering approach) is developed and applied on the K-means and on the the newly proposed Partially-Hidden Markov Model (PHMM). The results of the latter are shown to be closer to the expectations than the former.

As perspectives, several tracks are currently tackled:

- How to automatically set-up the window's size in the cluster filtering process? Various experiments let us think that one solution is to consider the level of energy released during the experiment. To make it more reliable, a combination with other features should be used.
- How to obtain a better description of some particular damages and a better discrimination of the mechanisms of a same damage family, such as ply delamination and splitting, in order to improve the interpretation of the damage process? The labelling process allowed in PHMM can be exploited to emphasize some kind of "macro-states" and a hierarchical processing of these macro-states could give some useful information about finer degradations.
- On the opposite to the previous item, given a large number of clusters representing micro-states, how to gather them into families of damages? Partially supervised learning in PHMM can be exploited to assign uncertain and imprecise prior on some waveforms about their membership to some predefined macro-states. The PHMM could then be applied to estimate if "components" have to be gathered (Serir, Ramasso, & Zerhouni, 2011).
- How to exploit the model-based approach (Rabiei, Modarres, & Hoffman, 2011) jointly with data-driven ones using possibly distributed sensors (Daigle, Bregon, & Roychoudhury, 2011) for a better health assessment and prognostics (Kessler, Flynn, Dunn, & Todd, 2011)? Many information fusion tools were developed in the literature (Ramasso & Jullien, 2011; Ramasso, Rombaut, & Zerhouni, 2012) and experiments are now necessary for a validation on composite structure analysis presented in this paper.

REFERENCES

Barr, S., & Benzeggagh, M. (1994). On the use of acoustic emission to investigate damage mechanisms in glass-fibre-reinforced polypropylene. *Composite Science Technology*, *52*, 369-376.

Come, E., Oukhellou, L., Denoeux, T., & Aknin, P. (2009). Learning from partially supervised data using mixture models and belief functions. *Pattern Recognition*, *42*(3), 334-348.

Daigle, M., Bregon, A., & Roychoudhury, I. (2011). Distributed damage estimation for prognostics based on structural model decomposition. In *Annual conference of the prognostics and health management society* (Vol. 2).

Dempster, A. (1967). Upper and lower probabilities induced by multiple valued mappings. *Annals of Mathematical Statistics*, *38*, 325-339.

Denoeux, T. (1995). A k-nearest neighbor classification rule based on Dempster-Shafer theory. *IEEE Trans. on Systems, Man and Cybernetics*, *5*, 804-813.

Denoeux, T. (2011). Maximum likelihood estimation from uncertain data in the belief function framework. *IEEE Transactions on Knowledge and Data Engineering*.

Ely, T., & Hill, E. (1995). Longitudinal splitting and fiber breakage characterization in graphite epoxy using acoustic emission data. *Mater. Eval.*, *53*, 369-376.

Hadzor, T. J., Barnes, R. W., Ziehl, P. H., Xu, J., , & Schindler, A. K. (2011, June). *Development of acoustic emission evaluation method for repaired prestressed concrete bridge girders* (Tech. Rep. No. FHWA/ALDOT 930-601-1). 238 Harbert Engineering Center, Auburn, AL 36849: Auburn Highway Research Center, Department of Civil Engineering.

Huang, M., Jiang, L., Liaw, P., Brooks, C., Seeley, R., & Klarstrom, D. (1998). Using acoustic emission in fatigue and fracture materials research. *Journal of Materials*, *50*(11), 1-12. (The Minerals, Metals & Materials Society (TMS))

Huguet, S. (2002). *Application de classificateurs aux donnees d'emission acoustique: identification de la signature acoustique des mecanismes d'endommagement dans les composites a matrice polymere*. Unpublished doctoral dissertation, Institut national des sciences appliquees (Lyon), Groupe dEtudes de Metallurgie Physique et de Physique des Materiaux. (in French)

Huguet, S., Godin, N., Gaertner, R., Salmon, L., & Villard, D. (2002). Use of acoustic emission to identify damage modes in glass fibre reinforced polyester. *Composite Science Technology*, *62*, 1433-1444.

Kessler, S. S., Flynn, E. B., Dunn, C. T., & Todd, M. D. (2011). A structural health monitoring software tool for optimization, diagnostics and prognostics. In *Annual conference of the prognostics and health management society* (Vol. 2).

Klir, G., & Wierman, M. (1999). Uncertainty-based information. elements of generalized information theory.

In (chap. Studies in fuzzyness and soft computing). Physica-Verlag.

Momon, S., Godin, N., Reynaud, P., RMili, M., & Fantozzi, G. (2012). Unsupervised and supervised classification of ae data collected during fatigue test on cmc at high temperature. *Composites Part A: Applied Science and Manufacturing*, *43*, 254-260.

Momon, S., Moevus, M., Godin, N., RMili, M., Reynaud, P., Fantozzi, G., et al. (2010). Acoustic emission and lifetime prediction during static fatigue tests on ceramic-matrix composite at high temperature under air. *Composites Part A: Applied Science and Manufacturing*, *41*, 913-918.

Rabiei, M., Modarres, M., & Hoffman, P. (2011). Structural integrity assessment using in-situ acoustic emission monitoring. In *Annual conference of the prognostics and health management society.*

Rabiner, L. (1989). A tutorial on hidden Markov models and selected applications in speech recognition. *Proc. of the IEEE*, *77*, 257-285.

Ramasso, E., Denoeux, T., & Zerhouni, N. (2012). Partially-Hidden Markov Models. In *International conference on belief functions.* Compiegne, France. (Accepted in February 2012)

Ramasso, E., & Jullien, S. (2011). Parameter identification in Choquet integral by the Kullback-Leibler divergence on continuous densities with application to classification fusion. In *European society for fuzzy logic and technology* (p. 132-139). Aix-Les-Bains, France.

Ramasso, E., Rombaut, M., & Zerhouni, N. (2012). Joint prediction of observations and states in time-series based on belief functions. *IEEE Transactions on Systems, Man and Cybernetics - Part B: Cybernetics*. (Accepted (http://dx.doi.org/10.1109/TSMCB.2012.2198882))

Serir, L., Ramasso, E., & Zerhouni, N. (2011). Time-sliced temporal evidential networks: the case of evidential hmm with application to dynamical system analysis. In *Ieee int. conf. on prognostics and health management* (p. 1-10). Denver, CO, USA.

Serir, L., Ramasso, E., & Zerhouni, N. (2012). Evidential evolving gustafson-kessel algorithm for online data streams partitioning using belief function theory. *International Journal of Approximate Reasoning*, *5*, 747-768.

Shafer, G. (1976). *A mathematical theory of Evidence*. Princeton University Press, Princeton, NJ.

Smets, P. (1994). What is Dempster-Shafer's model ? In I. R. Yager, M. Fedrizzi, & J. Kacprzyk (Eds.), *Advances in the dempster-shafer theory of evidence* (p. 5-34). J.Wiley & Sons.

Smets, P., & Kennes, R. (1994). The Transferable Belief Model. *Artificial Intelligence*, *66*(2), 191-234.

Vannoorenberghe, P., & Denoeux, T. (2002). Handling uncertain labels in multiclass problems using belief decision trees. In *Information processing and management of uncertainty in knowledge-based systems* (p. 1919-1926).

Vannoorenberghe, P., & Smets, P. (2005). Partially supervised learning by a Credal EM approach. In *Europ. conf. on symbolic and quantitative approaches to reasoning with uncertainty* (Vol. 3571, p. 956-967).

Wang, Y. (2011). Multiscale uncertainty quantification based on a generalized hidden markov model. *Journal of Mechanical Design*, *133*, 031004(1-10).

Zhou, W., Kovvali, N., Reynolds, W., Papandreou-Suppappola, A., Chattopadhyay, A., & 20, J. . D. Cochran vol., pp. 1271-1288. (2009). On the use of hidden markov modeling and time-frequency features for damage classification in composite structures. *Journal of Intelligent Material Systems and Structures, Special Issue on Information Management in Structural Health Monitoring*, *20*, 1271-1288.

Zhou, W., Reynolds, W., Moncada, A., Kovvali, N., Chattopadhyay, A., Papandreou-Suppappola, A., et al. (2008). Sensor fusion and damage classification in composite materials. In *Proc. spie* (Vol. 69260N).